

Amplification and switching functions of SOA: impact of amplified spontaneous emission noise

ENGY K. EL NAYAL^a, HEBA A. FAYED^b, AHMED ABD EL-AZIZ^b, MOUSTAFA H. ALY^{b,#,*}

^aElectrical Engineering Department, Faculty of Engineering, Pharos University, Alexandria, Egypt

^bPhotonic Research Lab (PRL) Electronics and Communications Engineering Department, College of Engineering and Technology, Arab Academy for Science, Technology and Maritime Transport, Alexandria, Egypt,

[#]Member of OSA

This paper proposes the segmentation model of the travelling wave-semiconductor optical amplifier (TW-SOA) or simply (SOA) including the impact of the amplified spontaneous emission (ASE) noise, which is the most important key characteristics that has a clear impact on its performance. The model is used to analyze the direct effects of the input parameters (input pulse power, bias current and input signal wavelength) on the signal gain. These important parameters used to characterize the SOA are represented in case of launching a single Gaussian pulse and also a packet of pulses. This investigation introduces the optimized conditions required for the SOA to maximize its gain for amplification and also to optimize its nonlinear characteristics when used in optical switching.

(Received June 15, 2015; accepted September 9, 2015)

Keywords: Carrier density, semiconductor optical amplifier (SOA), amplified spontaneous emission (ASE) noise

1. Introduction

With the tremendous growth of the Internet and the large increase in traffic demands, the necessity of new generation optical networks for managing the high-speed data flows has appeared. One of the most promising technologies for high bit rate optical networks is the semiconductor optical amplifier (SOA) [1].

The SOA is an optical gain device that can be used for different optical applications like wavelength converters, optical switches, signal regenerators as well as optical logic gates, which lead to improve the performance in optical network equipment. Most of these functionalities are based on the nonlinear effects of the SOA as the cross-gain modulation (XGM), self-phase modulation (SPM), the cross-phase modulation (XPM) and the four wave mixing (FWM) [1-8].

One of the major aspects is to consider the amplified spontaneous emission (ASE) noise because it strongly affects the SOA performance. The main source of noise in a semiconductor optical gain medium is the spontaneous emission of photons by recombination of electron-hole pairs. A number of schemes have been proposed to evaluate the optical signal to noise ratio (OSNR) and the noise figure (NF) of SOAs theoretically and experimentally [1, 9, 10]. Different approaches have been used to describe the ASE noise effects on the quality of the optically generated signals [11].

This paper addresses the impact of the ASE noise and its effect on the behavior and performance of the SOA focusing on the signal gain. This gain is dependent on the input parameters. The SOA parameters are investigated under the influence of ASE noise. The SOA length is 500

µm as commonly used [12, 13]. This study has a direct impact on the amplification and switching processes and hence achieves the desired improvement for best SOA performance.

This paper is organized as follows; in Sec. 2, the mathematical SOA segmentation model that accounts for the ASE noise is introduced. In Sec. 3, the significant input parameters that have a direct impact on the performance of SOA are investigated for both the amplification and switching processes. This is followed by conclusions and findings of this investigation in Sec. 4.

2. Mathematical model

When light is injected into the SOA, changes occur in the carrier density within the active region which can be described using the rate equations. These rate equations in small segments in a bulk InGaAsP/InP SOA are calculated while taking the carrier density changes into account [14].

The change in the carrier density within the active region is given by [15, 16]

$$\frac{dN}{dt} = \frac{I}{q.V} - (A.N + B.N^2 + C.N^3) - \frac{\Gamma.g(N,f).P_{av}.L}{V.h.f} - \frac{2\Gamma}{h.H.W} \sum_{j=0}^{N_m-1} \frac{g(N,v_j).k_j}{v_j} P_{ASE} \quad (1)$$

where I is the DC current injected to the SOA, q is the electron charge, V is the active volume of the SOA, Γ is the confinement factor, K_j is the filter factor, h is the Planck's constant, f is the light frequency, A is the nonradiative recombination coefficient due to the defects

and traps while B and C are the radiative and Auger recombination coefficients, respectively.

The material gain coefficient $g(N, \lambda)$ depends on both the carrier density, N, and the input signal wavelength, λ , is given by [16]

$$g(N, \lambda) = a_1(N - N_0) - a_2(\lambda - \lambda_N)^2 + a_3(\lambda - \lambda_N)^3 \quad (2)$$

where a_1 is the differential gain parameter, a_2 and a_3 are empirically determined constants, N_0 is the carrier density at the transparency point. λ_N is the peak gain wavelength, given by [15]

$$\lambda_N = \lambda_0 - a_4(N - N_0) \quad (3)$$

where λ_0 is the peak gain wavelength at transparency and a_4 denotes the empirical constant.

The average output power, P_{av} , over the length of the SOA can be expressed by [15]

$$P_{av} = \frac{1}{L} \int_0^L P_{in} \cdot G \, dz \quad (4)$$

where L is the length of the SOA, P_{in} is the input signal power and G is the total gain of an optical wave experienced at a location z of an SOA. The total gain can be calculated according to [15]

$$G = e^{g_T \cdot z} \quad (5)$$

where g_T is the net gain coefficient defined by

$$g_T = \Gamma \cdot g(N, f) - \alpha_s \quad (6)$$

where α_s is the internal waveguide scattering loss.

P_{ASE} is the amplified spontaneous emission noise power. It obeys the travelling-wave equation [16]

$$\frac{dP_{ASE}}{dz} = (\Gamma g(N, \nu_j) - \alpha_s) P_{ASE} + R_{sp} \quad (7)$$

where R_{sp} represents the local spontaneously generated noise and is given by [16]

$$R_{sp} = \Gamma \cdot g(N, \nu_j) \cdot \Delta \nu_m \cdot h \cdot \nu_j \quad (8)$$

The spontaneous emission distributes itself continuously over a relatively wide band of wavelengths with random phases between adjacent wavelength components. These noise photons frequencies ν_j are given by [16]

$$\nu_j = \nu_c + j \Delta \nu_m, \quad j = 0 \dots (N_m - 1) \quad (9)$$

where N_m is a positive integer, ν_c ($= E_{go}/h$) is the cut-off frequency and $\Delta \nu_m$ is the longitudinal mode frequency spacing given by

$$\Delta \nu_m = \frac{c}{2 n_{eq} L} \quad (10)$$

where c is the speed of light in vacuum and n_{eq} is the equivalent index of the amplifier waveguide.

E_{go} , the bandgap energy with no injected carriers, is given by the quadratic approximation [17]

$$E_{go} = q (a' + b' y + c' y^2) \quad (11)$$

where a' , b' and c' are the quadratic coefficients and y is the molar fraction of Arsenide in the active region.

The above model which involves dividing the SOA into fifty segments is executed via Matlab™ and the physical SOA parameters used are given in Table 1.

Table 1 Physical parameters used in this work [18].

Parameter	Value
Carrier density at transparency (N_0)	$1.4 \times 10^{24} \text{ m}^{-3}$
Wavelength at transparency (λ_0)	1605 nm
Initial carrier density (N_i)	$3 \times 10^{24} \text{ m}^{-3}$
Internal waveguide scattering loss (α_s)	$40 \times 10^2 \text{ m}^{-1}$
Differential gain (a_1)	$2.78 \times 10^{-20} \text{ m}^{-2}$
Gain constant (a_2)	$7.4 \times 10^{18} \text{ m}^{-3}$
Gain constant (a_3)	$3.155 \times 10^{25} \text{ m}^{-4}$
Gain peak shift coefficient (a_4)	$3 \times 10^{-32} \text{ m}^4$
SOA Length (L)	500 μm
SOA width (W)	3 μm
SOA height (H)	80 nm
Confinement factor (Γ)	0.3
Filter factor (k_f)	1
Bandgap energy quadratic coefficient (a')	1.35
Bandgap energy quadratic coefficient (b')	- 0.775
Bandgap energy quadratic coefficient (c')	0.149
Nonradiative recombination coefficient (A)	$3.6 \times 10^8 \text{ s}^{-1}$
Radiative recombination coefficient (B)	$5.6 \times 10^{-16} \text{ m}^3/\text{s}$
Auger recombination coefficient (C)	$3 \times 10^{-41} \text{ m}^6/\text{s}$
Equivalent refractive index (n_{eq})	3.5
Facet reflectivities (R_1, R_2)	0
Differential of equivalent refractive index with respect to carrier density (dn/dN)	$- 1.2 \times 10^{-26} \text{ m}^{-3}$
Molar fraction of Arsenide in active region (y)	0.892

3. Results and discussions

3.1 Optimum performance of SOA for amplification function

The important role that SOA plays in almost functions within all-optical routers is amplification. So, this section aims to present the optimum performance of SOA as an amplifier. For the SOA to execute as an amplifier, the input signal should not be affected by the nonlinear response due to the gain saturation. The amplification can be achieved if the gain does not reach its stable saturation level when applying an input pulse. For maximum

amplification, it is important to control the point at which the peak gain is maximum.

3.1.1 Effect of ASE noise on a single pulse

The direct impact of the ASE noise on the signal gain for a single propagating Gaussian pulse and also a packet of pulses are highlighted in this section. When a short input pulse with 1 mW peak power and 1.1667 ps width is injected to the SOA, this results in an instant drop in the SOA gain due to the interaction of this pulse with the excited electrons in the conduction band. The gain depletion due to ASE noise reaches a lower value compared to noise free propagation. The output response for Gaussian pulse with and without ASE is displayed in Fig. 1. The impact of the ASE noise has reduced the 232 mW peak power to 217 mW.

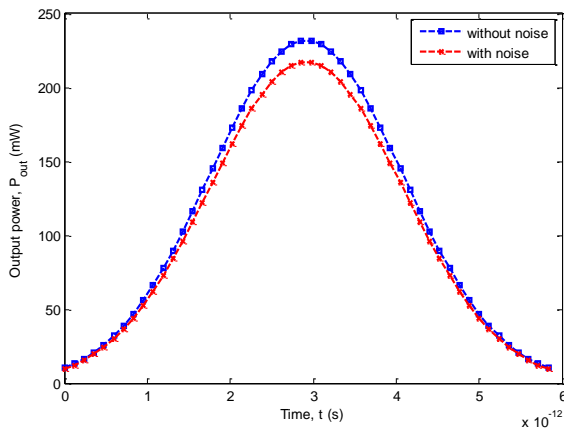


Fig. 1. Impact of ASE noise.

This gain depletion is dependent on the input peak power of the signal. The impact of the ASE noise on the SOA gain for the range of input peak power ($1 \text{ mW} < P_p < 50 \text{ mW}$) at 150 mA and 1550 nm is executed in Fig. 2.

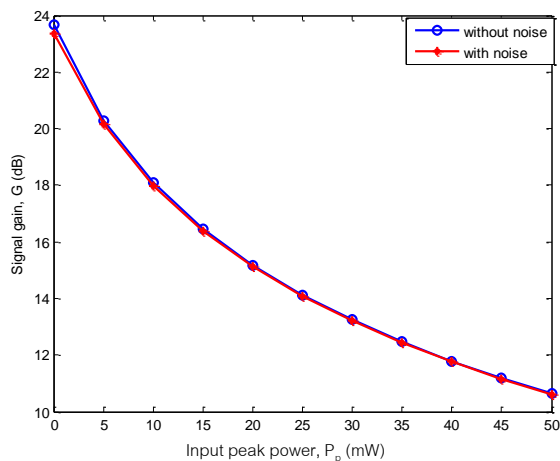


Fig. 2. Signal gain response as a function of the input peak power

As seen, the SOA drop gain is reduced with the input power. The reason for such response is that, the signal with higher power level will interact with a larger number of excited electrons in the conduction band. This results in a higher depletion of the carrier density and consequently leads to drop in the SOA gain. A maximum signal gain of 22.6 dB and 22.85 dB is achieved at the optimum peak power of 1 mW for an input Gaussian signal with and without noise, respectively.

The effect of wavelengths in the C-band (1530 to 1565 nm) on the signal gain difference is shown in Fig. 3. It is clear that, the signal gain is higher at smaller values of input power at all wavelengths. The highest gain drops (i.e., maximum impact of ASE noise) are, respectively, 9.3535 dB, 10.2464 dB and 8.8487 dB, corresponding to 7.5369 %, 5.4959 % and 4.5470 % percentage gain drop at 1530, 1550 and 1565 nm. On the other hand, the lowest gain drops at the same wavelengths are -13.60 dB, -16.32 dB and -12.81 dB corresponding to 0.4778 %, 0.2018 % and 0.3660 %, respectively. It is noticed also that, there is a common peak power of 6 mW between these wavelengths to give the same signal gain difference of 4.6 dB.

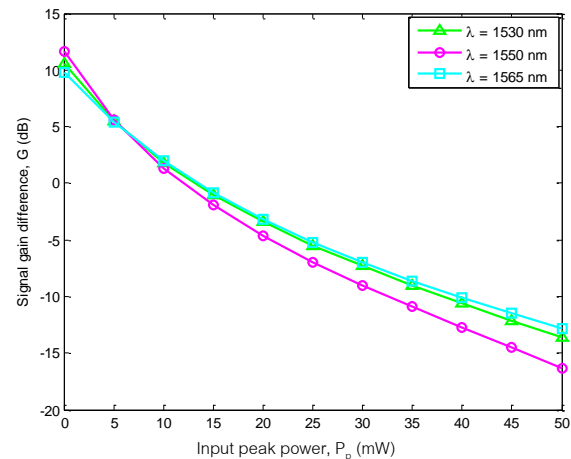


Fig. 3. Signal gain difference as a function of the input peak power at different values of the input signal wavelengths

As shown in Fig. 2, the depletion of the gain that occurs due to the injection of the input pulse is directly related to the input power. Also, the wavelength of the input pulse has a direct impact on the SOA gain as it can be seen from the gain coefficient, Eq. (2). For this reason, the signal gain with and without ASE noise against all values of the input signal wavelengths included in the C-band is displayed in Fig. 4 at 1 mW which is the optimum input peak power. This figure shows that the depletion of SOA gain due to the input pulse propagation is wavelength dependent. Moreover, it depicts the relationship between the gain and the bandwidth of the amplifier.

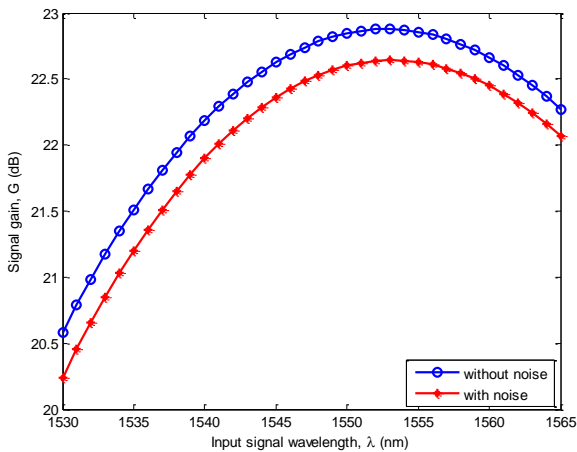


Fig. 4. SOA drop gain response against input signal wavelength with and without ASE noise

It is clear that, at any input power, the gain has a peak value within its bandwidth at a wavelength λ_N and decays at both ends from this particular wavelength. These peak gains are observed around 1550-1560 nm. So, at each value of the peak power, there is an optimum signal wavelength corresponding to the highest value of gain. The highest drop gain values with and without noise are, respectively, 22.64 dB and 22.88 dB at 1553 nm.

The effect of the input signal power, P_p , on the peak gain wavelength, λ_N , is displayed in Fig. 5.

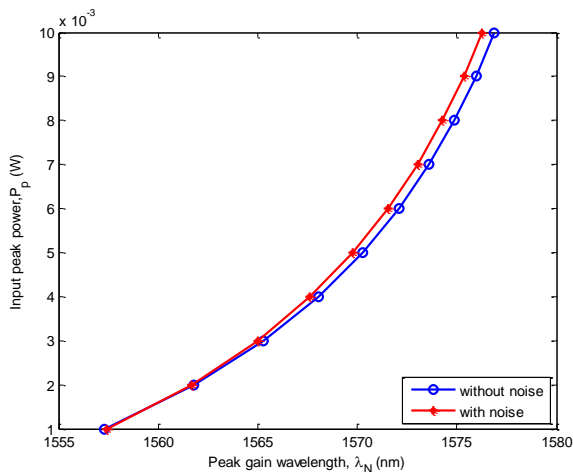


Fig. 5. Input peak power against peak gain wavelength

This figure shows a linear shift in the peak gain wavelength against the input signal power. Higher input powers result in more depletion of the SOA gain and consequently an increased peak gain wavelength as observed. At 1 mW of input pulse power the peak gain wavelength is 1557 nm in the presence of ASE noise.

The signal gain drop for the input signal, when ASE noise is considered, is depicted in Fig. 6 at different bias

currents. At $\lambda = 1550$ nm, the gain drops are 10.25, 11.97 and 9.145 dB, i.e., 5.496 %, 2.032 % and 0.6032 % drops, at 150, 200 and 250 mA, respectively.

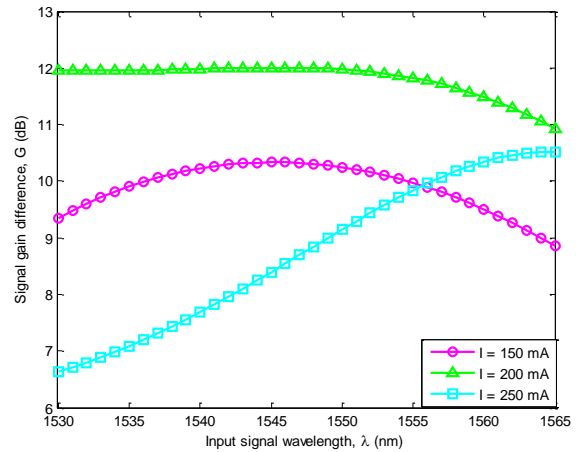


Fig. 6. Signal gain difference as a function of the input signal wavelengths at different biasing current

Now, the investigation now is carried out to study the obvious effect of the applied (biasing) current on the SOA gain, Fig. 7.

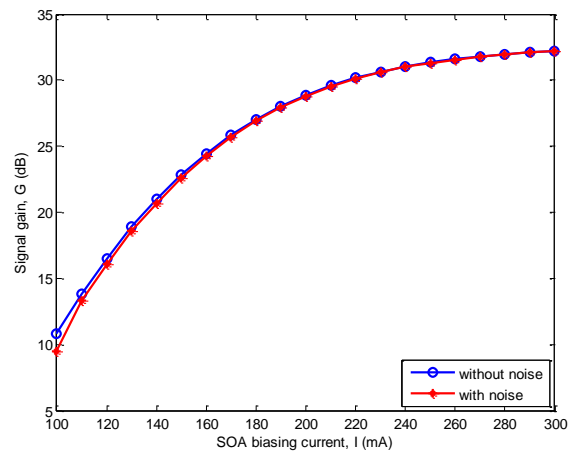


Fig. 7. Signal gain against bias current

Fig. 7 shows the relation between the signal gain and the biasing current in the range 100-300 mA at $\lambda = 1550$ nm. This response is depicted at the lowest input peak power of 1 mW to achieve the optimum maximum gain.

As shown in Fig. 7, at higher bias current, the number of electrons overcoming the energy gap increases (i.e., carrier density increases), leading to increase the SOA total gain. When applying a biasing current 50 mA, the signal gain is 22.60 dB and 22.85 dB, with and without ASE, while the higher biasing current 300 mA achieves a

higher gain of 32.23 dB and 32.24 dB with and without noise, respectively. These results correspond to the number of electrons available for amplification in the conduction band for each case.

The difference in the SOA drop gain for the input signal is displayed in Fig. 8 with the biasing current. For 150 and 300 mA, the gain drops are 10.25 dB and 5.211 dB which correspond to drops of 5.496 % and 0.1984 %, respectively.

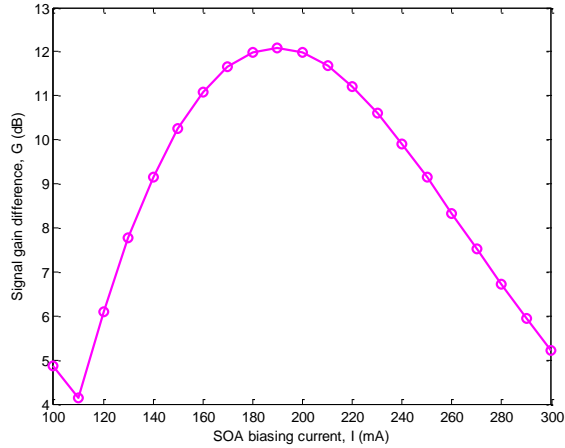


Fig. 8. Signal gain difference against biasing current

The effect of the biasing current on the peak gain wavelength is depicted in Fig. 9. It is noted that, the peak gain wavelength is increased at lower biasing currents. This is seen at 150 mA, where the peak gain wavelength is ~ 1561 nm in the presence of ASE noise. On the other hand, when the SOA is injected by higher bias currents, higher number of electrons is excited in conduction band and hence the SOA gain achieves higher values. As a result, λ_N decreases.

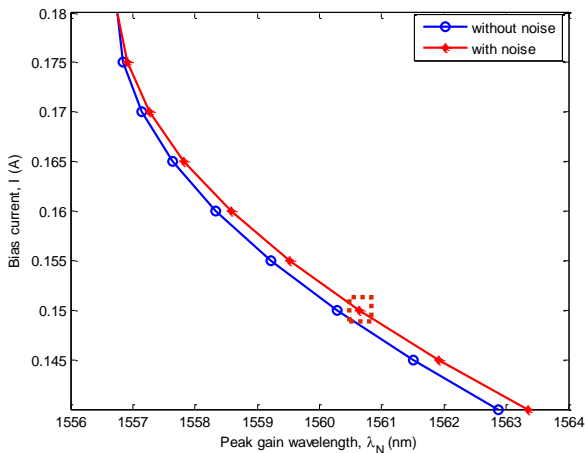


Fig. 9. Bias current as a function of the peak gain wavelength with and without noise

3.1.2 Effect of ASE noise on a sequence of pulses

The investigation now is re-illustrated with and without ASE noise for a sequence of pulses or a packet. The burst consists of 10 Gaussian pulses, each of which is identical to the one investigated earlier. All pulses are separated by 100 ps (i.e., 10 Gbps data rate) for 1 ns packet duration.

The response of the average burst gain to the input peak power, at 1550 nm and at a stable biasing current of 150 mA, is similar to Fig. 2 but with different values. However, the average gains of the pulses within the packet are less than the gains of the single propagating pulse with and without the ASE noise. This is due to the further gain depletions to the SOA gain in case of packet propagation. A maximum burst gain, with and without noise, respectively, of 21.8860 dB and 22.1117 dB is achieved at the optimum input peak power of 1 mW.

Also, the same response of Fig. 3 is obtained for the burst gain difference at the three investigated wavelengths, but the highest gain drops here are 8.3897 dB, 9.1555 dB and 8.0627 dB which correspond to 6.9624 %, 5.0628 % and 4.3019 % percentage gain drop at 1 mW peak power, respectively. Otherwise, at peak power of 50 mW, the lowest gain drops are -9.4573 dB, -9.0975 dB and -5.8106 dB, i.e., 1.7213 %, 1.4499 % and 2.6395 %, respectively.

Furthermore, the investigation is proceeded to study the effect of all values of the input signal wavelengths included in the C-band on burst gain. It is found that, the optimum signal wavelength which gives the highest value of burst gain is 1553 nm. 21.95 dB and 22.17 dB are the highest drop burst gain obtained with and without ASE noise, respectively.

The burst gain difference versus all wavelengths at 150, 200, 250 mA bias currents is shown in Fig. 10. At $\lambda = 1550$ nm, the differences are 9.156, 10.33 and 9.044 dB (5.0628 %, 1.9564 % and 0.8503 %), respectively.

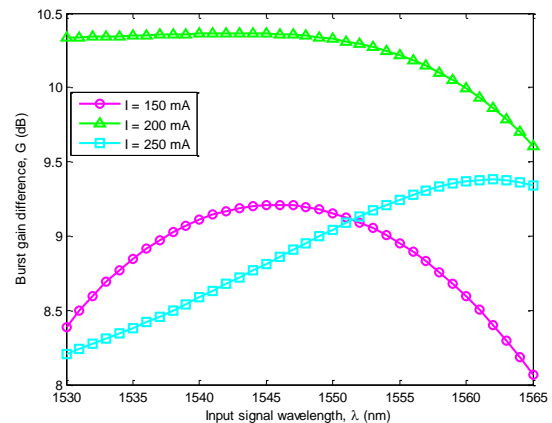


Fig. 10. The burst gain difference as a function of the input wavelength at different values of the biasing current

To show the effect of the biasing current on the average burst gain, the response of Fig. 7 repeats itself

again but with lower values. At 150 mA, the burst gain achieved is 21.89 dB and 22.11 dB, while the higher current of 300 mA gives 30.88 dB and 30.90 dB with and without noise, respectively.

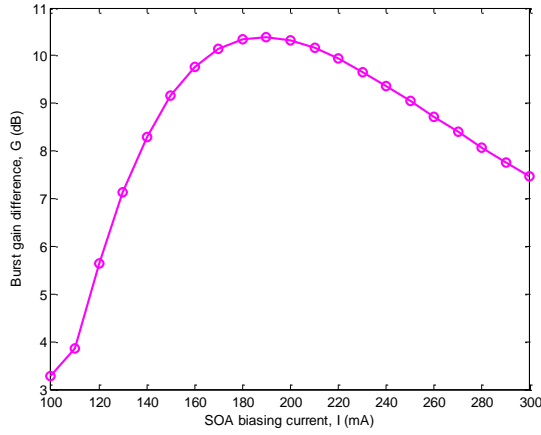


Fig. 11. Burst gain difference versus the biasing current

Moreover, the difference in the burst drop gain for the input packet is displayed in Fig. 11 at all currents. For 150 and 300 mA, the gain drops are 9.156 dB and 7.459 dB, i.e., 5.0628 % and 0.4524 %, respectively.

3.2 Optimum performance of SOA for switching

Another important function that SOA plays within all-optical routers is switching. On the contrary to amplification, the XPM characteristic is used for the SOA to execute this process. So, the input signal should experience a phase shift of 180° for the complete deconstructive interference [19]. Therefore, the investigation in this section introduces the boundaries necessary for the input parameters to achieve the 180° induced phase shift for managing this function.

Due to the propagation of the input pulse through the SOA, changes in the carrier density take place, affecting its propagation coefficient (via the nonlinear refractive index variations in the SOA active region). This leads to SPM to occur at which the leading edge of the input pulse experiences a different phase shift relative to the lagging edge [16, 17]. Δn represents the effective refractive index variation within the active region [16]

$$\Delta n = \Gamma \frac{dn}{dN} (N - N_{ss}) \quad (12)$$

where dn/dN is the refractive index shift coefficient and N_{ss} is the carrier density at steady state (i.e., with no input signal launched to SOA). The total phase shift experienced by the propagating input signal is [16]

$$\Delta\phi = \int_0^L \frac{2\pi}{\lambda} \Delta n. dz \quad (13)$$

As defined in the above equations, the phase shift experienced by a single propagating pulse, is directly proportional to the depletion of the carrier density, as a result of changes in the refractive index (Δn).

Fig. 12 shows the induced phase shift as a function of the input peak power at 1550 nm and at a stable bias current of 150 mA. The dotted line indicates at which value of the input peak power the destructive interference approximately attains 180° . It is found that, it occurs clearly when $P_p \approx 25$ mW (without noise) and ≈ 27 mW (with noise).

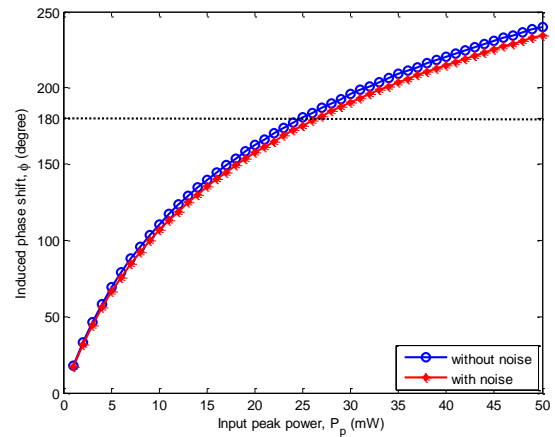


Fig. 12. Induced phase shift experienced by the input signal against the input peak power

Obviously, to perform the switching function, the optimum peak power chosen should be greater than 20 mW for an input signal.

The induced phase shift against all values of the input signal wavelengths included in the C-band is displayed in Fig. 13 for input peak power 25 mW and 30 mW. This is done to confirm that each input signal wavelength achieves 180° at a particular input peak power. Considering ASE noise, the destructive interference exactly occurs at 180.2° and 180.4° at 1554 and 1545 nm, respectively, for the same peak power values.

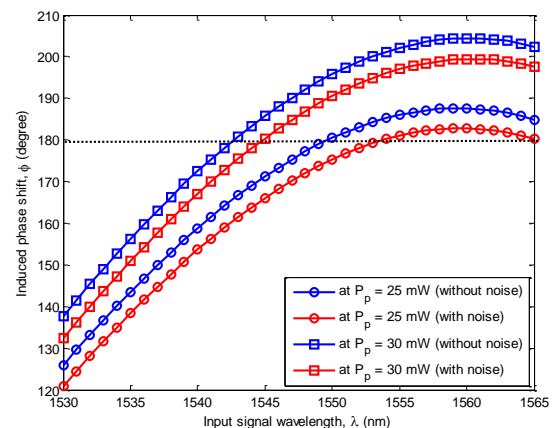


Fig. 13. Induced phase shift of the input signal versus the signal wavelength at 25 mW and 30 mW input peak power

Also, the bias current has a direct impact on the induced phase shift of the input signal. This is illustrated in Fig. 14 at a range of biasing current 100-300 mA.

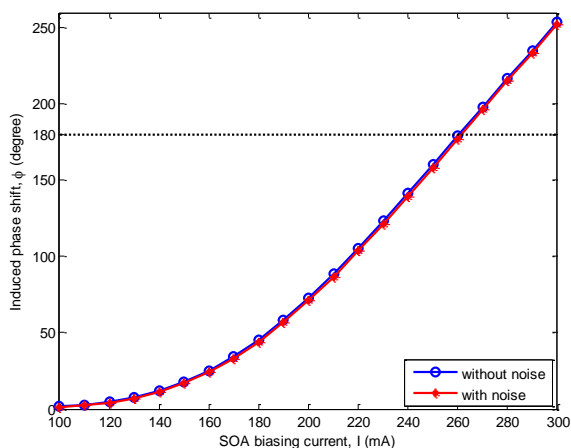


Fig. 14. Induced phase shift against the biasing current

It easily noted that, at higher bias currents, the input signal propagating along the SOA induces more phase shift. This is because the higher biasing current results in higher SOA gain which in turn results in more carrier density depletion and accordingly, a phase shift increase. It is also noted that, at 150 mA, no phase shift of 180° appears. This is because the peak power here is only 1 mW, which should be greater than 20 mW as explained earlier. But, at higher currents, 179° phase shift is achieved at 260 mA.

4. Conclusion

This paper has introduced the use of the SOA to perform as an amplifier and as a switch. The impact of the input pulse power, the applied biasing current and the input signal wavelength of the Gaussian pulse within the C-band is investigated to achieve the optimum performance of SOA for both functions under the influence of the ASE noise. A maximum gain of 22.6 dB and 21.886 dB is achieved with ASE noise at the optimum peak power of 1 mW, 150 mA and wavelength of 1550 nm for a single pulse and a burst of pulses, respectively.

Results obtained using the proposed segmentation model show that, the required SOA input parameters are necessary to achieve a 180° induced phase shift for the switching function. It was attained at 27 mW input peak power and at 150 mA and 1550 nm input signal wavelength.

References

[1] Y. Said, H. Rezig, A. Bouallegue, *The Open Optics Journal*, **2**, 61 (2008).

- [2] L. Guo, M. Connelly, *Optics Express*, **14**, 2938 (2006).
- [3] M. V. Drummond, L. N. Costa, R. N. Nogueira, P. Monteiro, A. Teixeira, *Proceeding of the 10th Anniversary International Conference on Transparent Optical Networks, ICTON 2008*, 106 (2008).
- [4] H. Zhaoyang, M. Davanco, D. J. Blumenthal, *IEEE Photonics Technology Letters*, **15**, 1419 (2003).
- [5] M. Jabbari, M. K. Moravvej-Farshi, R. Ghayour, A. Zarifkar, *J. Lightwave Technol.*, **27**, 2199 (2009).
- [6] L. K. Oxenlowe, D. Zibar, M. Galili, A. T. Clausen, L. J. Christiansen, P. Jeppesen, *Proceeding of Conference on Lasers and Electro-Optics Europe, CLEO/Europe 2005*, p. 486, 2005.
- [7] A. M. Clarke, G. Girault, P. Anandarajah, C. Guignard, L. Bramerie, L. P. Barry, J. C. Simon, J. Harvey, *Proceeding of the 19th Annual Meeting of the IEEE Lasers and Electro-Optics Society, LEOS 2006*, pp. 152-153, 2006.
- [8] D. Jianji, Z. Xinliang, X. Jing, H. Dexiu, F. Songnian, P. Shum, Z. Liren, Y. D. Gong, *Proceeding of the Conference on Optical Fiber Communication and the National Fiber Optic Engineers, OFC/NFOEC 2007*, pp. 1-3, 2007.
- [9] Guido Giuliani, Davide D'Alessandro, *J. Lightwave Technol.*, **18**(9), 1256 (2000).
- [10] E. Staffan Björlin, John E. Bowers, *IEEE Journal of Quantum Electronics*, **38**(1), 61 (2002).
- [11] Guohua Qi, Joe Seregelyi, Stéphane Paquet, J. Claude Bélisle, *Proc. SPIE 5971, Photonic Applications in Nonlinear Optics, Nanophotonics, and Microwave Photonics*, pp. 59712D.1-59712D.8, 2005.
- [12] R. Gutierrez-Castrejon, L. Schares, L. Occhi, G. Guekos, *IEEE Journal of Quantum Electronics*, **36**(12), 1476 (2000).
- [13] Prashant P. Baveja, Aaron M. Kaplan, Drew N. Maywar, Govind P. Agrawal, *Proc. SPIE 7598, 759817.1* (2010).
- [14] M. Hattori, K. Nishimura, R. Inohara, M. Usami, *J. Lightwave Technol.*, **25**, 512 (2007).
- [15] W. P. Ng, A. A. El Aziz, Z. Ghassemlooy, Moustafa H. Aly, R. Ngah, *IET Commun.*, **6**(5), 484 (2012).
- [16] H. Wang, J. Wu, J. Lin, *Journal of Optics A: Pure and Applied Optics*, **7**, 479 (2005).
- [17] M. J. Connelly, *Semiconductor Optical Amplifiers*, New York: Springer, Verlag, 2002.
- [18] VPIsystems, *VPI Transmission Maker and VPI Component Maker: Photonic Modules Reference Manual*, 2001.
- [19] M. F. Chiang, Z. Ghassemlooy, N. Wai Pang, H. Le Minh, A. A. El Aziz, *Proceeding of the IEEE International Conference on Communications, ICC '08.*, pp. 5321-5325, 2008.

*Corresponding author: drmosaly@gmail.com